

CONTACT PROBLEM FOR THE AUTOFRETTAGE OF THICK CYLINDERS

GENNADIY LVOV AND SERGEY LYSENKO
Kharkov Polytechnic University
310002 Kharkov, 21 Frunze Str., Ukraine
lvovgi@kpi.kharkov.ua

[Received: October 4, 2001]

Abstract. The autofrettage of thick-walled cylinders with variable thickness is considered on the basis of a variational formulation of the corresponding elastic-plastic contact problem. The numerical solution is determined by the use of the finite element method. We have chosen a material model which takes kinematic hardening and the ideal Baushinger effect into account. The optimum geometric parameters for the bandage and the initial gap are both determined in a way that a favorable distribution of residual stresses will develop and the bandage is removed after unloading.

Mathematical Subject Classification: 74M15, 74S0

Keywords: autofrettage, finite element method, contact problem, residual stresses

1. Introduction

Thick-walled cylinders subjected to high impulsive pressure are wide-spread as elements of many important constructions. When the magnitude of pressure is commensurable with the yield point of the material, a raise of strength can be reached by the special methods of the autofrettage. In an outcome of the intended plastic deformations caused by the interior pressure acting in the cylinders a favourable field of residual stresses is developed.

In works [1-3] the process of forming residual stresses is investigated for a broad class of materials with various types of deformation diagrams.

The magnitude of residual stresses depends on what sizes the areas of plastic deformations have and on the differences in character between the stress distributions in plastic and elastic conditions.

The possibilities for the autofrettage are frequently limited by the strength of the cylinders during plastic loading. Such a restriction is especially essential for cylinders with various wall thicknesses because the creation of irregular technological pressure for the autofrettage entails significant engineering difficulties.

It is expedient to apply technological bandages for restriction of strains of cylinders in areas with a smaller thickness of walls for raising the effectiveness of autofrettage

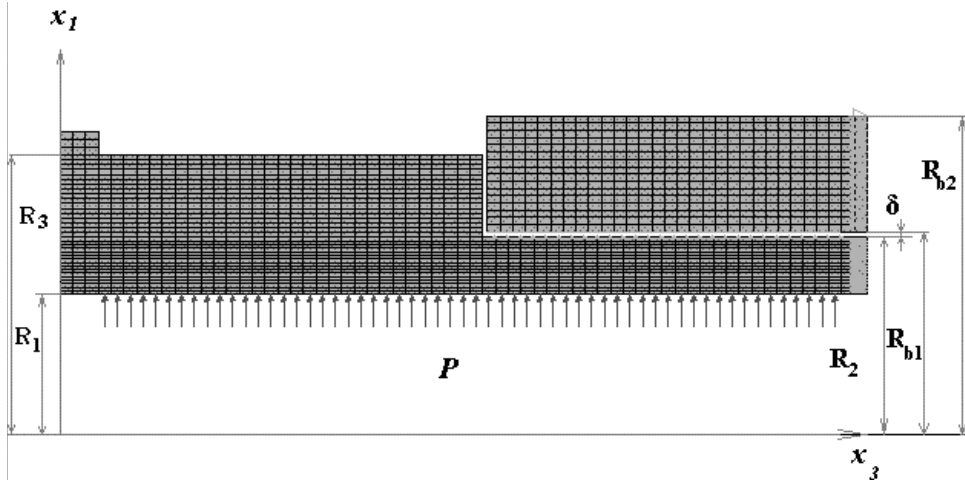


Figure 1. Finite element model of a composite construction

in cylinders of a variable thickness. The scheme of such an autofrettage with uniform pressure and one restraining bandage is shown in Figure 1.

2. Description of investigation of autofrettage

The theoretical analysis of a process of autofrettage is reduced to the solution of an elastic-plastic problem which includes loading and unloading by taking the contact interaction of the cylinder and technological bandage into consideration.

Let's consider such a problem for two bodies of revolution assuming axisymmetric deformations. During loading and unloading the stress increments $d\sigma_{11}, \dots, d\sigma_{13}$ of the deformed solid bodies should satisfy the equilibrium equations

$$\frac{\partial}{\partial x_1}(d\sigma_{11}) + \frac{\partial}{\partial x_3}(d\sigma_{31}) + \frac{d\sigma_{11} - d\sigma_{22}}{x_1} = 0, \quad (2.1a)$$

$$\frac{\partial}{\partial x_3}(d\sigma_{33}) + \frac{\partial}{\partial x_1}(d\sigma_{31}) + \frac{1}{x_1}d\sigma_{13} = 0. \quad (2.1b)$$

The surface S of each body can be presented as a union of two surfaces: $S = S_F \cup S_K$, where S_F is the surface on which the increments of the exterior forces are given, and S_K is the contact region between the cylinder and the bandage.

The exterior surface of the cylinder is given by the parametrical equations $x_1 = x_1(\alpha)$, $x_3 = x_3(\alpha)$, where α is the length of the meridian curve in initial condition.

The interior surface of the bandage, where contact is possible, is given by the equation $f(x_1, x_3) = 0$. The kinematic condition on the displacement increments dU_C and dU_B in the cylinder and bandage due to the interaction assumes the form of an inequality:

$$f(x_1, x_3) + \text{grad } f \cdot (U_C + dU_C) - \text{grad } f \cdot (U_B + dU_B) \leq 0. \quad (2.2)$$

Condition (2.2) is equality in the contact zone.

The strain increments $d\varepsilon_{11}, \dots, d\varepsilon_{13}$ are related to the displacements u_1, u_3 via linear equations:

$$d\varepsilon_{11} = \frac{\partial}{\partial x_1}(du_1), \quad d\varepsilon_{22} = \frac{1}{x_1}(du_1), \quad (2.3a)$$

$$d\varepsilon_{33} = \frac{\partial}{\partial x_3}(du_3), \quad d\varepsilon_{13} = \frac{1}{2} \left[\frac{\partial}{\partial x_1}(du_3) + \frac{\partial}{\partial x_3}(du_1) \right]. \quad (2.3b)$$

The deformation trajectories in the autofrettage processes have a complicated character. During unloading secondary plastic deformations may emerge with an opposite sign. Under the conditions of contact interaction the loading process will not be simple even for a monotone increase of the exterior load.

For an adequate description of the plastic deformations it is necessary to use physical relations reflecting the Baushinger effect and the directed character of hardening. As the physical relations satisfying the conditions mentioned for one cycle of loading and unloading we have selected the theory of plasticity with anisotropic hardening [4,5]. The increment of plastic deformations $d\varepsilon_{ij}^p$ is determined by the law

$$d\varepsilon_{ij}^p = d\lambda \cdot \frac{\partial \varphi}{\partial \sigma_{ij}}, \quad (2.4)$$

in which $d\lambda$ is a parameter to be determined,

$$\varphi = \frac{3}{2} (S_{ij} - \rho_{ij}) \cdot (S_{ij} - \rho_{ij}) - \sigma_y^2 = 0 \quad (2.5)$$

is the surface of plasticity, $S_{ij} = \sigma_{ij} - \delta_{ij}\sigma_0$ denotes the stress deviator (σ_0 is the first scalar invariant of the stress tensor), σ_y is the yield stress in the initial state. The character of directed hardening is determined by the deviator ρ_{ij} obtained from the accumulated plastic deformations:

$$\rho_{ij} = \int C(\varepsilon_i^p) d\varepsilon_{ij}^p. \quad (2.6)$$

The integral is calculated on the loading path. If C is constant the hardening is linear. The multilinear law of hardening corresponds to a discrete combination of the values $C_k(\varepsilon^p)$, where C_k has a constant value for every separate section of approximation for the deformation diagram.

The position of a surface of plasticity is determined by the history of plastic deformations, but the hardening is transmitted which corresponds to the ideal Baushinger effect.

The increment of plastic deformations can be given in terms of the stress increments

$$d\varepsilon_{ij}^p = \frac{(S_{mn} - \rho_{mn}) \cdot d\sigma_{mn}}{3 \cdot C \cdot (S_{kl} - \rho_{kl}) \cdot (S_{kl} - \rho_{kl})} (S_{ij} - \rho_{ij}). \quad (2.7)$$

If the conditions for active loading are not satisfied, the increment of plastic deformations is equal to zero.

For each stage of the autofrettage process determination of the displacement, stress and strain increments requires the integration of a boundary value problem defined by

the field equations (2.1), (2.3) and (2.7), which should be associated with appropriate boundary conditions and the kinematic restriction for the contact interaction (2.2).

The problem is a nonlinear one since during the solution it is necessary to determine the boundaries of the contact area and the character of loading for both cylinders.

For a numerical solution by the finite element method the problem is reduced to an extremum problem for a functional defined on the kinematically admissible displacement increments which should also satisfy inequality (2.2):

$$\min J(dU_C, dU_B) = \frac{1}{2} \iiint_{V_C + V_B} d\sigma_{ij} d\varepsilon_{ij} dV - \iint_{S_F} dU_C dp dS. \quad (2.8)$$

In this functional $d\varepsilon_{ij}$ is determined by the kinematic relations (2.3) and $d\sigma_{ij}$ is obtained from the inverse of relation (2.7). Equivalence of the extremum problem (2.8) to the contact problem follows from the theory of variational inequalities [6, 7].

3. Results

The numerical solution is determined by the finite element method for an axisymmetric autofrettage of the cylinder. The bandage has a cylindrical form. The initial geometric parameters of the construction have the following values (see Figure 1):

- the interior radius of cylinder $R_1 = 0.06$ m;
- the exterior small radius of cylinder $R_2 = 0.092$ m;
- the exterior large radius of cylinder $R_3 = 0.138$ m;
- the interior radius of bandage $R_{b1} = 0.093$ m;
- the exterior radius of bandage $R_{b2} = 0.16$ m;
- the length of cylinder $L = 0.525$ m; the length of bandage $L_b = 0.247$ m;
- the initial gap between the surfaces of the cylinder and bandage $\delta = 0.001$ m.
- the residual gap between the surfaces of the cylinder and bandage $\beta = 0.052$ mm.

The finite element model of the composite construction is made of axisymmetric solid elements with four nodal points which have two degrees of freedom (U_{x1}, U_{x3}). The coordinate x_3 corresponds to the rotational axis, and the coordinate x_1 is measured in the radial direction. The second order shape functions are used. For modelling the contact interaction between the surfaces of the cylinder and bandage, which in the initial non-loaded condition are separated by a gap δ , the axisymmetric three-nodal contact elements of the type "a knot to a surface" were used. The contact surface is modelled with the help of the pseudo-element technology. This surface can interact during the elasto-plastic loading and unloading. In Figure 1 the finite element model is shown. This includes 2058 axisymmetric elements (1538 for the cylinder and 480 for bandage), and also 38 contact elements between surfaces of the cylinder and the bandage.

The technological autofrettage process is produced by the interior hydraulic pressure exerted on the inner surface of the cylinder.

For carrying out the computations we have chosen the following data for the materials of the cylinder and bandage: modulus of elasticity $E = 0.21 \cdot 10^6$ MPa; Poisson's constant $\nu = 0,29$; yield stress $\sigma_y = 1200$ MPa; the strength $\sigma_B = 1500$ MPa. The deformation diagram $\sigma(\varepsilon)$ is assumed to be multilinear. The four sections of the diagram are given by point: $\sigma_k = 1200, 1400, 1500, 1900$ MPa; $\varepsilon_k = 0,0057, 0,02, 0,05, 0,43$.

The step by step loading of the cylindrical pipe by pressure autofrettage was applied in an interactive procedure with adjusting the loading steps automatically to solve the physically and structurally non-linear problem. In addition, we have assumed that the load follows a linear law in each step. Such a solution procedure for non-linear problems ensures fast convergence of the Newton-Raphson method (from 3 up to 10 iterations) and makes it possible to reflect the history of loading.

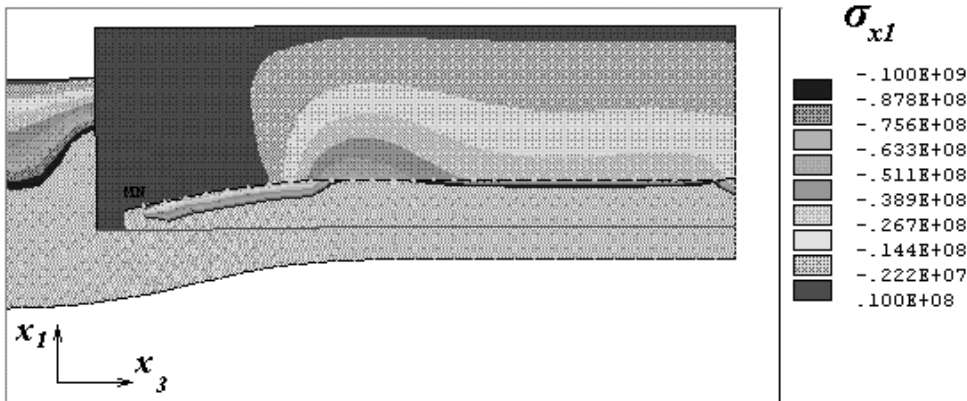


Figure 2. Distribution of radial stresses.

When one considers the contact autofrettage of the cylinders with the use of auxiliary bandages, one of the principal problems is to find the most appropriate values for the initial gap and the geometric parameters of the bandage. If the value of the initial gap meets the condition $\delta > 0.002$ m and the cylinder has a smaller thickness ($h = 0.032$ m) dangerous residual plastic deformations – up to 10% – can develop. In this case the bandage does not keep the strains under a reasonable limit. If the initial gap is too small ($\delta < 0.0007$ m), the residual plastic deformations in the cylinder prevent the full unloading in the bandage, therefore a residual pressure develops between the bandage and cylinder. Then the bandage cannot be removed from the cylinder. Moreover, the magnitude of the initial gap should ensure the release of the surfaces of the cylinder and bandage after unloading taking the residual gap β into consideration. Increasing the exterior radius of the bandage up to $R_{b2} = 0.192$ m, it is possible to significantly redistribute the stresses acting on the contact surfaces and to achieve a more uniform distribution of the residual radial displacements on the same surfaces after unloading. However, numerical experiments have shown that a big increase in the bandage thickness $h > 0.1$ m is ineffective. A repeated variation

of the geometric parameters resulted in the values: $\delta = 0.001$ m, $R_{b1} = 0.093$ m, $R_{b2} = 0.16$ m, which seem to be the best for an appropriate autofrettage.

The computational results we are going to present have all been obtained by the use of the above mentioned best parameters.

In the interactive regime of the computations of an autofrettage, seven loading conditions of the construction from the initial pressure $D = 500$ MPa up to a maximum value $D = 950$ MPa are fixed.

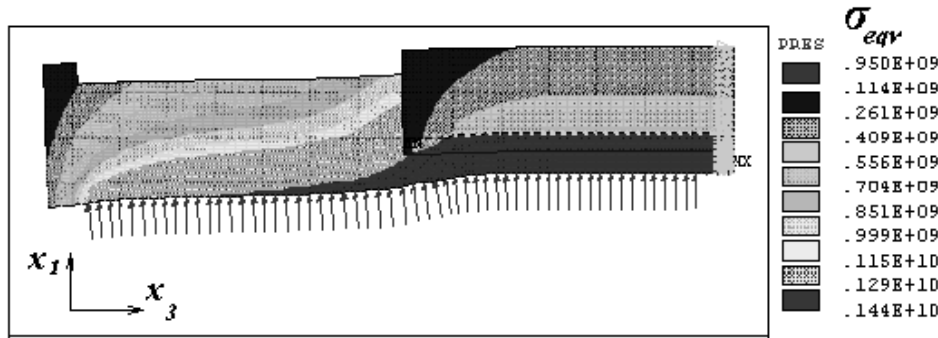


Figure 3. Distribution of equivalent stresses under of $P=950$ MPa

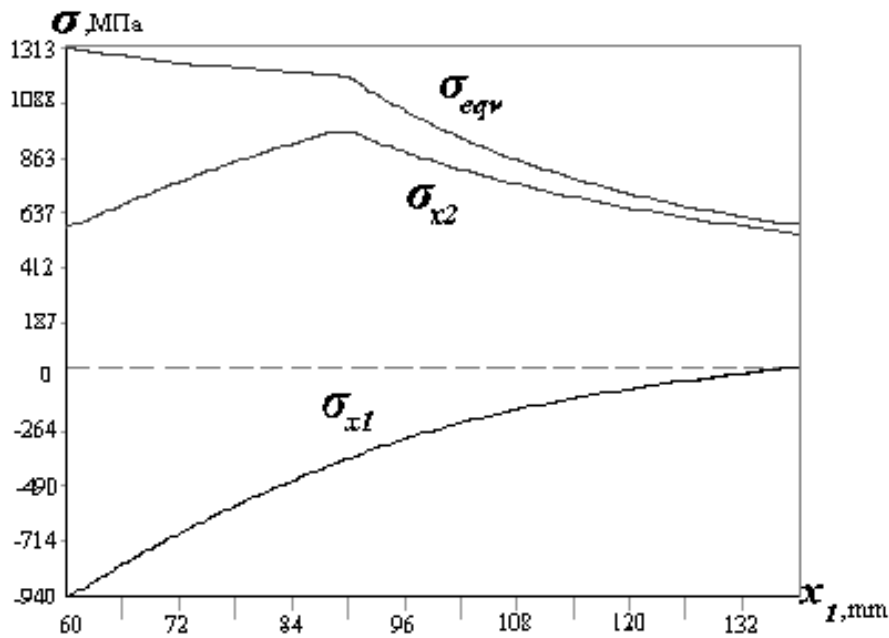


Figure 4. Distribution of stresses in the 1st cross-section

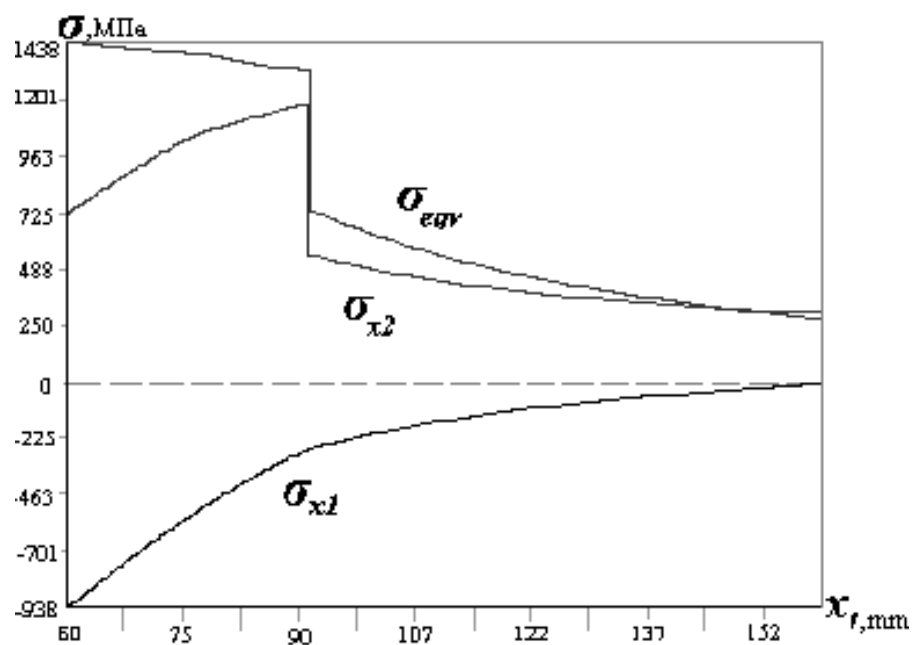
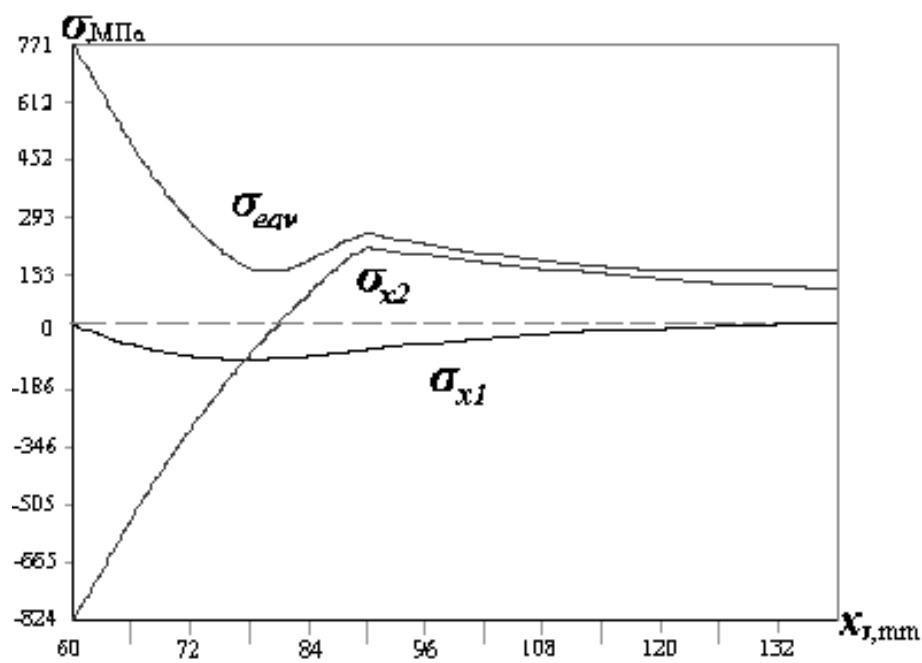


Figure 5. Distribution of stresses in the 2nd cross-section

Figure 6. Distribution of residual stresses in the 1st cross-section for $P = 0$

Under the initial load the zones of plastic deformation in the second part of the cylinder are small and the surfaces of the cylinder and bandage do not contact yet. Contact zones appear if the load reaches the value $P = 650$ MPa.

For $P = 700$ MPa, Figure 2 shows the zone of contact interaction. The final distribution of the Mises equivalent stresses when the construction is subjected to the maximum load $P = 950$ MPa is represented in Figure 3. It is seen from those level lines of stresses which reached the yield stress of the material $\sigma_y = 1200$ MPa that the second part of the cylinder is in a plastic condition, while in the first one it is less than 600 MPa. As the character of the stress distributions in the two parts they are significantly different and for this reason it is expedient to investigate the regularities of the stress distributions along the thickness in the cross-sections: 1) $x_3 = 0.15$ m; 2) $x_3 = 0.4$ m.

Figure 4 shows the distributions of the equivalent σ_{eqv} , circular σ_{χ_2} and radial σ_{χ_1} stresses due to the maximum load $P = 950$ MPa for the first cross-section. The same stresses are given in the second cross-section, which passes through the cylinder and the bandage (Figure 5). If the circular stresses are discontinuous on the common boundary of the bodies, the radial stresses are continuous.

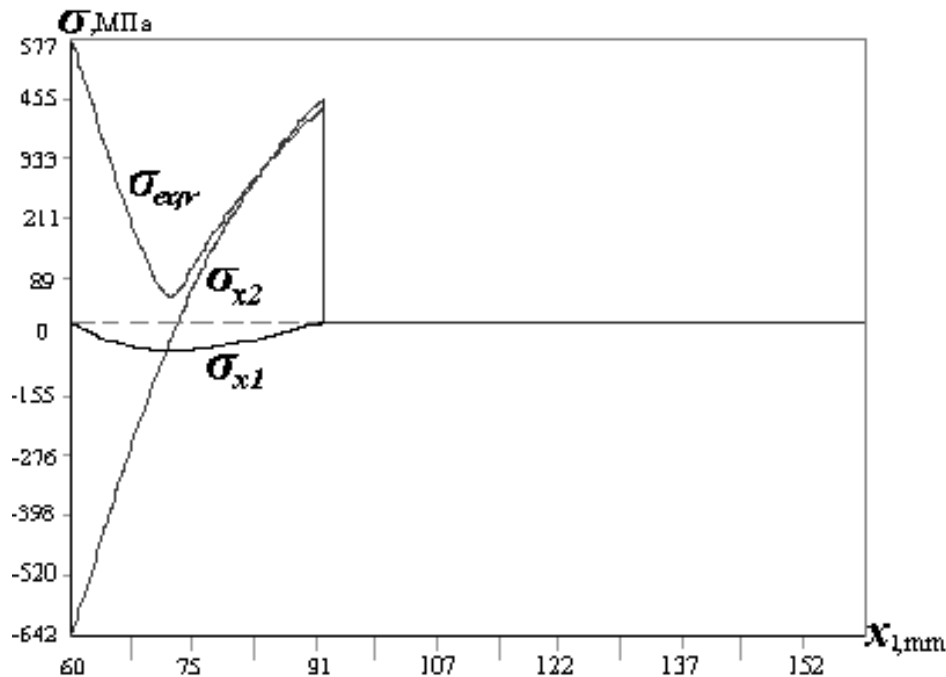


Figure 7. Distribution of the residual stresses in the 2nd cross-section for $P = 0$

In the last step the load was completely removed. Figure 6 shows the distribution of the residual stresses in the first cross-section. The circular stress reaches its maximum

$|\sigma_{X2}| = 824.5$ MPa on the interior surface of the cylinder. As regards the second cross-section (Figure 7), the stress distributions essentially differ and the circular stress on the interior surface has a sizeable magnitude $\sigma_{X2} = -642$ MPa. The distribution of the equivalent residual stresses is shown for the whole structure in Figure 8. The bandage is completely unloaded and the residual radial displacements on the exterior contact surface of the pipe in the second cross-section are less than the initial gap: $U_{X1} = 0.938$ mm. Then the actual gap after unloading is $\delta = 0.062$ mm, which exceeds the supposed value β , therefore the bandage can be removed from the cylinder.

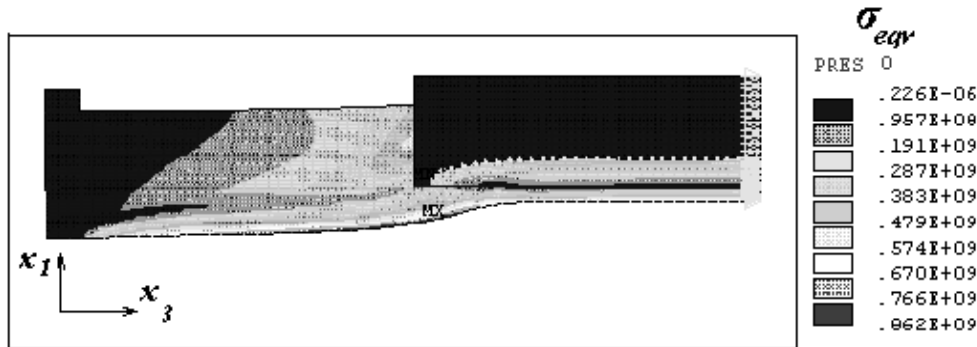


Figure 8. Distribution of equivalent residual stresses

4. Conclusions

The results of the study allow us to project of autofrettage processes for real elements of constructions which have a complex shape. On the basis of these results the parameters can be calculated for loading and technology tools which do not admit of failure of construction. The procedure we have presented allows us to determine rational parameters for the contact autofrettage under which highly uniform fields of residual stresses on the interior surface of the cylinder are achieved.

REFERENCES

1. BIRGER, I. A.: *Residual Stresses*, M., 1963, p. 230.
2. PERL, M. and ARONÉ, R.: *Stress intensity factors for a radially multicroaked partially-auto-frettagged pressurized thick-walled cylinder*, Trans. of the ASME, J. of Pressure Vessel Technology, **110**, (1988), 147 - 154.
3. SCHINDLER, H. J.: *Determination and evaluation of residual stresses in thick-walled cylinders due to auto-frettage*, Proc. of the 6th Int. Conf. on Residual Stresses, Oxford, U.K., July 10-12, 2000, Vol. 2, 837-844.
4. BALTOV, A. and SAWCZUK A.: *A rule of anisotropic hardening*, Acta Mechanica, **1**, (1965), 81-92.

5. KADASHEVICH, U. I. and NOVOZHILOV, V. V.: *A theory of plasticity which takes residual microstresses into account*, Applied Mathematics and Mechanics, **22**(1), (1958), 78-89. (in Russian).
6. DUVAUT, G. and LIONS, J. L.: *Inequalities in mechanics and physics*, Dunod, Paris, 1972. (in French).
7. LVOV G. I.: *Variational formulation of a contact problem for linearly elastic and physically non-linear slanting shells*, Applied Mathematics and Mechanics, **46**(5), (1982), 841-846. (in Russian).